RAY TRACING IN THE SMOOTHED ACOUSTIC SEG/EAGE SALT MODEL. PART 1: SEISMOGRAMS

VÁCLAV BUCHA

Department of Geophysics, Faculty of Mathematics and Physics, Charles University, Ke Karlovu 3, 121 16 Praha 2, Czech Republic, bucha@seis.karlov.mff.cuni.cz

ABSTRACT

Two-point rays of refracted and reflected P-waves in the smoothed acoustic SEG/EAGE Salt Model are computed. The shot-receiver configuration is derived from the original SEG/EAGE Phase A Acquisition. The square of 21x21 receivers and three shots are used to compute rays. One profile is used to generate the ray-theory seismograms. The calculations demonstrate that the smoothed SEG/EAGE Salt Model is suitable for two-point ray tracing.

KEY WORDS

Velocity model, ray tracing, seismic waves, synthetic seismograms

INTRODUCTION

The greatest advantages of ray tracing in comparison with precise methods, e.g., finite differences, finite elements, are the speed of computation, the small memory requirements and the possibility to separate elementary seismic waves. The original 3-D SEG/EAGE Salt Model is a very complex model and cannot be directly used for ray tracing, because ray tracing computations need smooth velocity macro models (Bucha et al., 2003). Is the smoothed SEG/EAGE Salt Model suitable for two-point ray tracing computations?

All computations were performed on a PC with the Linux operating system. The GOCAD program was used to visualize the 3-D smoothed Salt Model with shots, receivers and computed rays.

SMOOTHED ACOUSTIC SEG/EAGE SALT MODEL

The Salt Model selected for ray tracing computations was smoothed by Bulant (2001, 2002, 2003). It is the best model obtained as a result of many test smoothing computations. The model is parameterized by B-splines and was smoothed using Sobolev scalar products. The smoothed Salt Model is composed of the most important interfaces and velocity blocks. The interfaces, which are characterized by the highest discontinuities in the velocity field, are the ocean bottom, the interfaces limiting the salt body, the geopressure horizon and the bottom flat interface (see Figure 1). The velocity blocks are the water (velocity is constant), the background above the geopressure horizon (three-dimensionally varying velocity), the salt (velocity is constant), the background below the geopressure horizon (three-dimensionally varying velocity) and the bottom half space (velocity is constant).

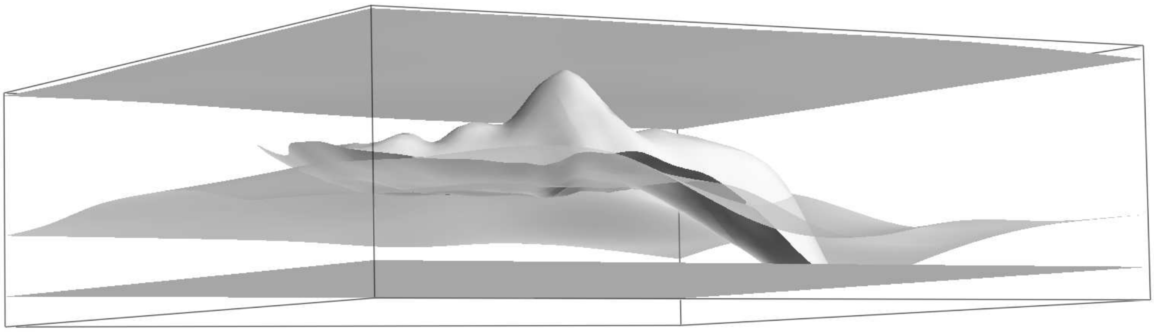

Figure 1. Smoothed Salt Model with the most important interfaces: ocean bottom, interfaces limiting the salt body, geopressure horizon, bottom flat interface. The geopressure horizon is partially transparent.

SHOTS AND RECEIVERS

The position of shots and receivers is derived from the original Phase A Acquisition SEG/EAGE (Aminzadeh et al., 1997). Three shots are used to compute the rays. One shot (sphere on Figure 2) is located at the centre of the square of 21 x 21 receivers above the salt crest at a depth of 20m. Figure 2 shows the location of the well (diamond) near the centre of the square of 21 x 21 receivers. Two shots are located in the well, one shot above the salt body, at a depth of 900m, and the other shot below the salt body, at a depth of 2300m.

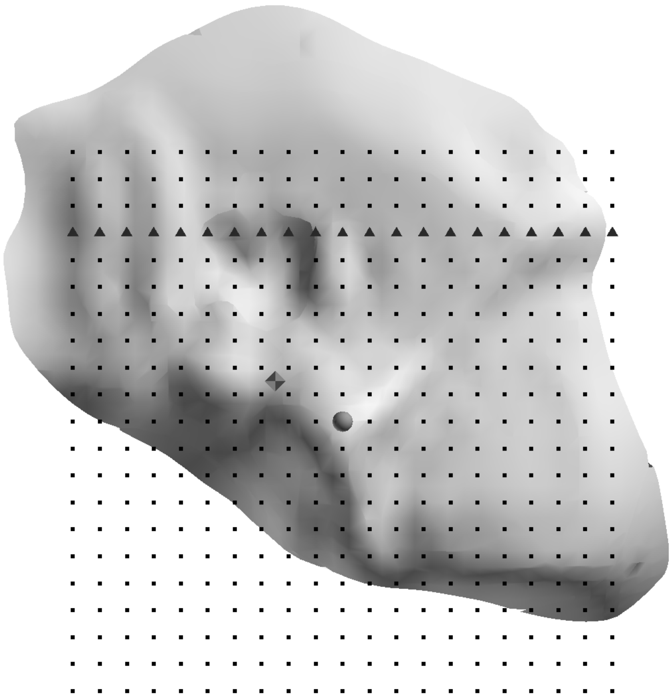

Figure 2. Top view of the salt body, shot point, well and receiver points. The sphere in the centre of configuration is the shot at the depth of 20m. The diamond represents the well with two shots similar to the original Phase A Acquisition. One profile (tetrahedrons) is used to generate synthetic seismograms.

The square of 21 x 21 receivers is located above the salt body (see Figure 2). The receivers are located at a depth of 0m and the grid interval is 320m, which seems to be reasonable for computation and visualization. The receiver grid interval in the Phase A Acquisition was 20m. An attempt to compute one elementary wave for the grid of 329x329 receivers with an interval of 20m was successful, but the sizes of the output files make the visualization of rays difficult. The seismograms along the profile denoted by tetrahedrons are displayed in Figures 7, 8, 9.

RAY TRACING COMPUTATIONS

The two-point rays of refracted and reflected P-waves are determined by means of the two-parametric shooting method using the MODEL, CRT and FORMS subroutine packages (Červený et al., 1996). The salt model is a complex model and the intersection of the geopressure interface with the salt body required the use of several elementary waves in computing the P-waves reflected from the top and bottom of the salt body and from the bottom interface.

Two-point rays of one refracted and three reflected P-waves are computed for the shot located above the salt crest at the depth of 20m and for the shot in the well, above the salt, at the depth of 900m. Reflections are calculated from the top and bottom interfaces limiting the salt body and from the bottom flat interface. Eight elementary waves are defined.

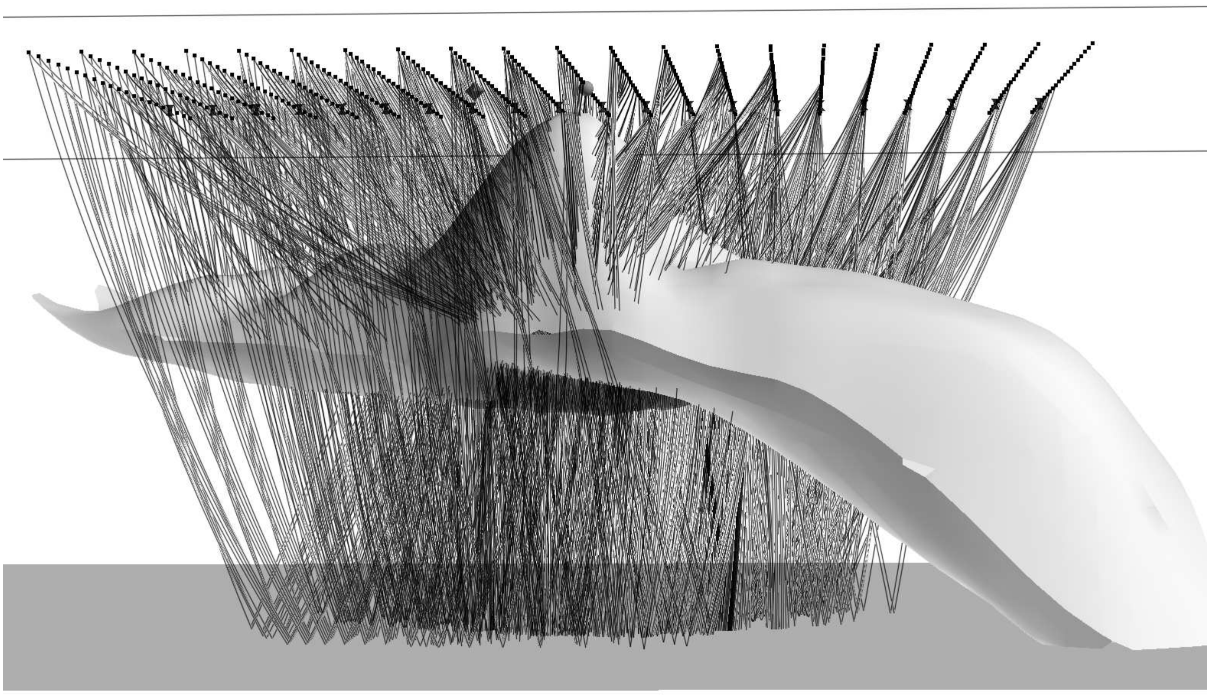

Figure 3. Rays of P-wave reflected from the bottom flat interface. The shot is located at the centre of the square of 21x21 receivers, above the salt crest, at a depth of 20m.

The two-point rays of one refracted and four reflected P-waves (three of them are multiply reflected) are computed for the shot in the well, below the salt body, at the depth of 2300m. The single reflection comes from the bottom interface. Multiple

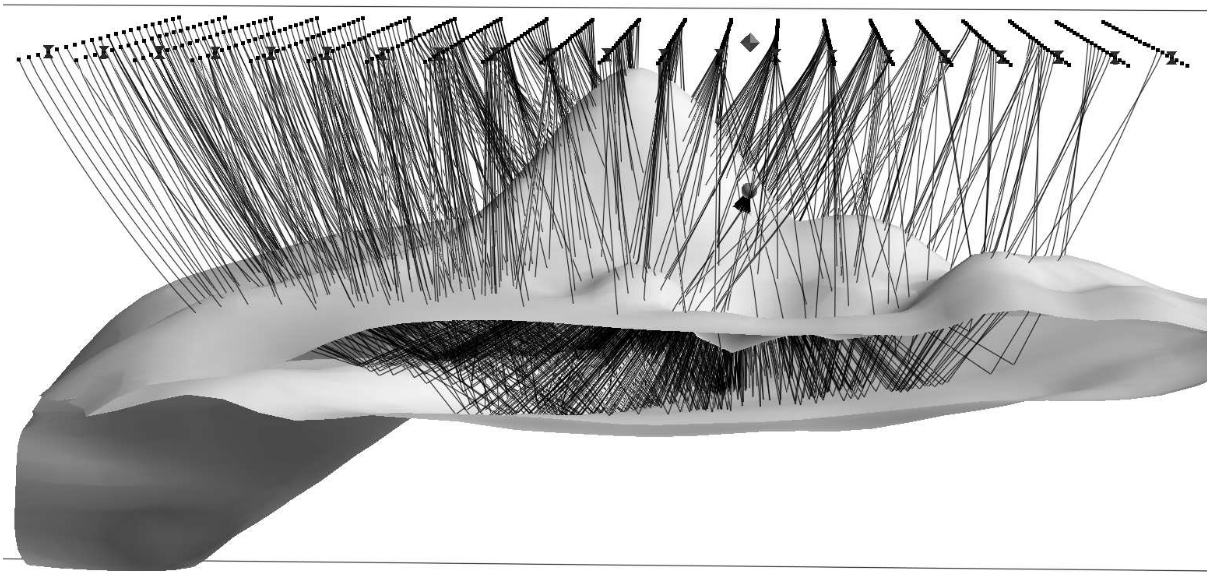

Figure 4. Rays of P-wave reflected from the bottom interface limiting the salt body. The shot is located in the well, above the salt, at a depth of 900m. The model is cut by the GOCAD slicer.

reflections are from the top and bottom of the salt body, from the bottom of the salt and bottom flat interface, from the top of the salt and bottom flat interface. Twelve elementary waves are defined.

Figures 3, 4, 5 and 6 show the two-point rays of the computed waves. The figures are screen snapshots of several GOCAD camera positions.

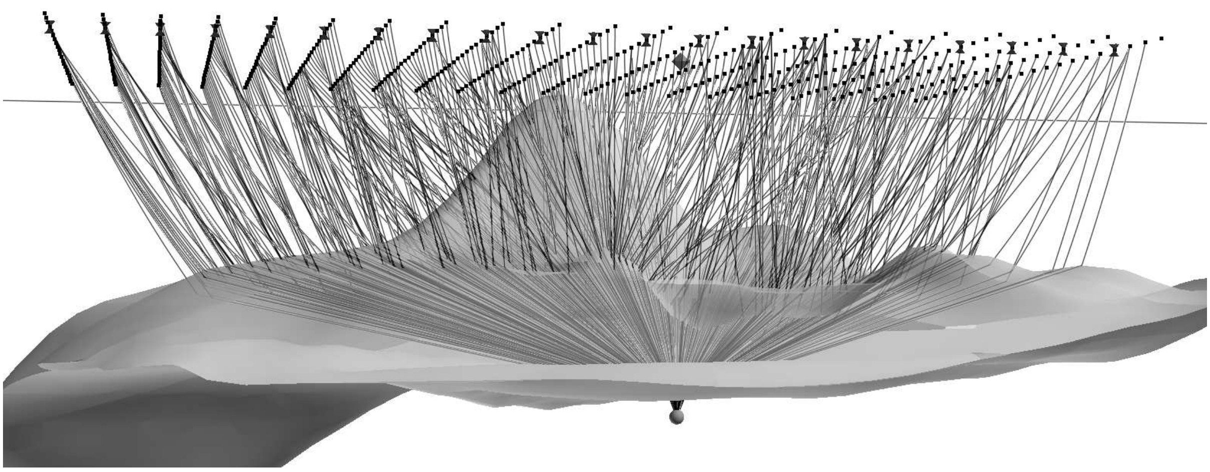

Figure 5. Rays of the refracted P-wave. The shot is located in the well, below the salt, at a depth of 2300m. The salt top interface is partially transparent.

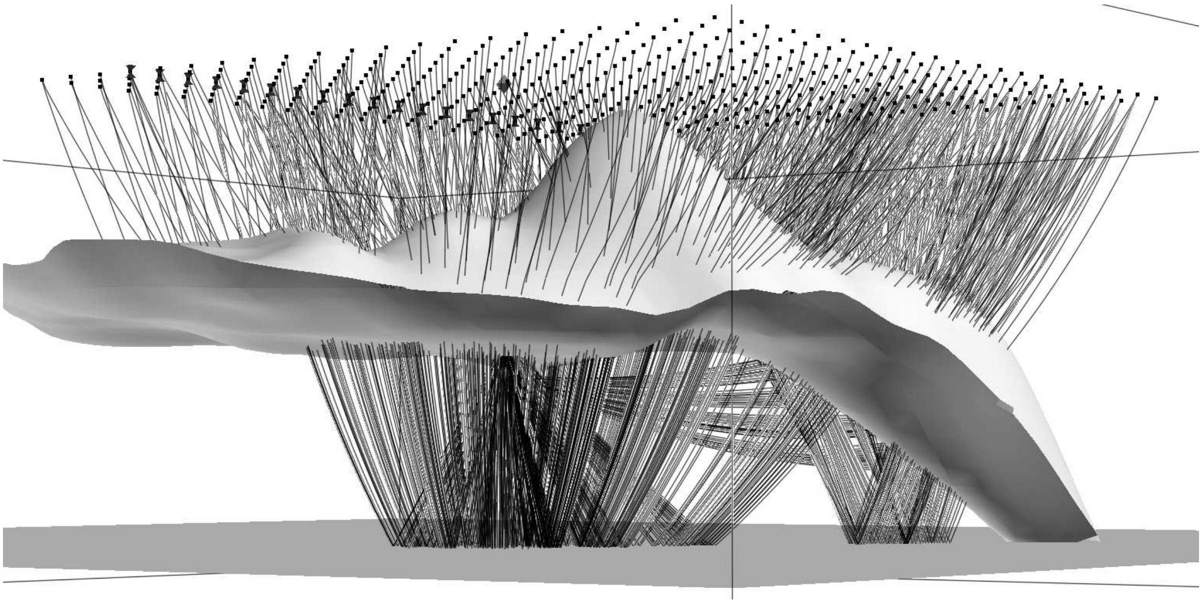

Figure 6. Rays of the P-wave multiply reflected from the bottom of the salt and from the bottom flat interface. The shot is located in the well, below the salt, at a depth of 2300m.

SYNTHETIC SEISMOGRAMS

One profile, selected from the 21 x 21 square grid of receivers, was used to generate the ray-theory seismograms in the frequency domain. The selected profile is marked by tetrahedrons in Figure 2. The source time function is defined by the Gabor signal, prevailing frequency 30Hz. The source is an isotropic explosion. The output of the ray-tracing program is converted to elementary Green functions, and the frequency-domain response function is calculated. The synthetic seismograms are then computed and plotted. The amplitudes of the ray-theory seismograms are not correct because free-surface conversion coefficients are not considered.

The vertical components of the ray-theory seismograms for the three shots are plotted in Figures 7, 8 and 9. Figure 7 corresponds to the shot located above the salt crest at the depth of 20m, Figure 8 shows seismograms for the shot located in the well, above the salt body, at the depth of 900m, and Figure 9 corresponds to the shot in the well, below the salt body, at the depth of 2300m. Figures 7a, 8a and 9a show the seismograms generated from all the computed elementary waves. The maximum amplitude of each trace is scaled to a given constant. Figures 7b, 8b and 9b show travel times of the individual elementary waves distinguished by centred symbols.

The travel times of the individual elementary waves (Figures 7b, 8b, 9b) and simultaneous visualization of the model interfaces, rays, shots and receivers should help to interpret the seismograms generated from all the computed elementary waves (Figures 7a, 8a, 9a). For example, Figure 9 shows seismograms for the shot in the well at the depth of 2300m located near the salt bottom interface. The arrival times of the wave reflected from the bottom flat interface and the wave multiply reflected from the bottom salt and the bottom flat interface are close. This multiply reflected wave is called the ghost. Both waves are clearly visible in Figure 9b.

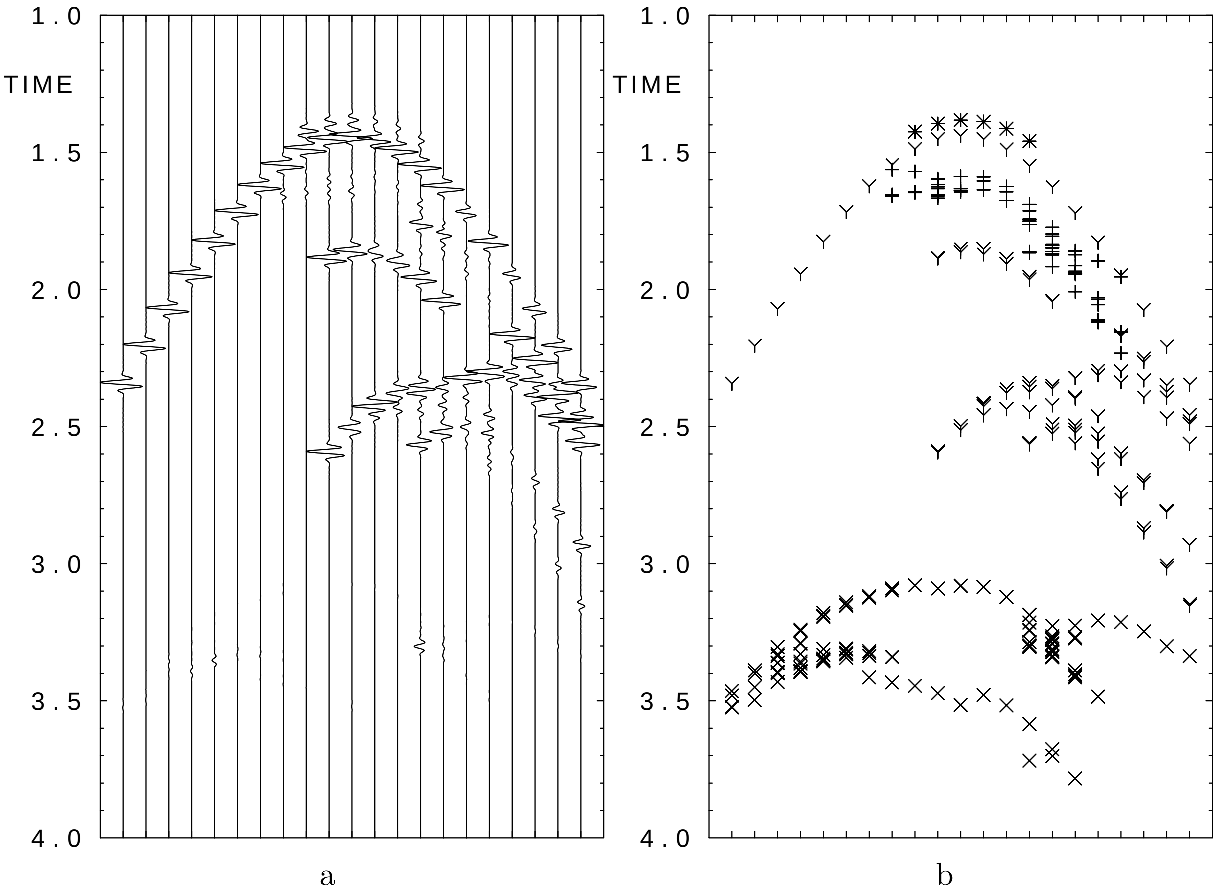

Figure 7. Shot located at the centre of the square of 21 x 21 receivers above the salt crest at a depth of 20m. **a**: Vertical components of synthetic seismograms of all computed elementary waves along the selected profile. The amplitudes of each trace are scaled according to the maximum amplitude of each trace. **b**: Travel times of the individual elementary waves along the selected profile. ' $*$ ' denotes the refracted wave, ' Y ' denotes the reflections from the top of salt, ' $+$ ' denotes the reflections from the bottom of salt and ' $\times$ ' denotes the reflections from the bottom interface.

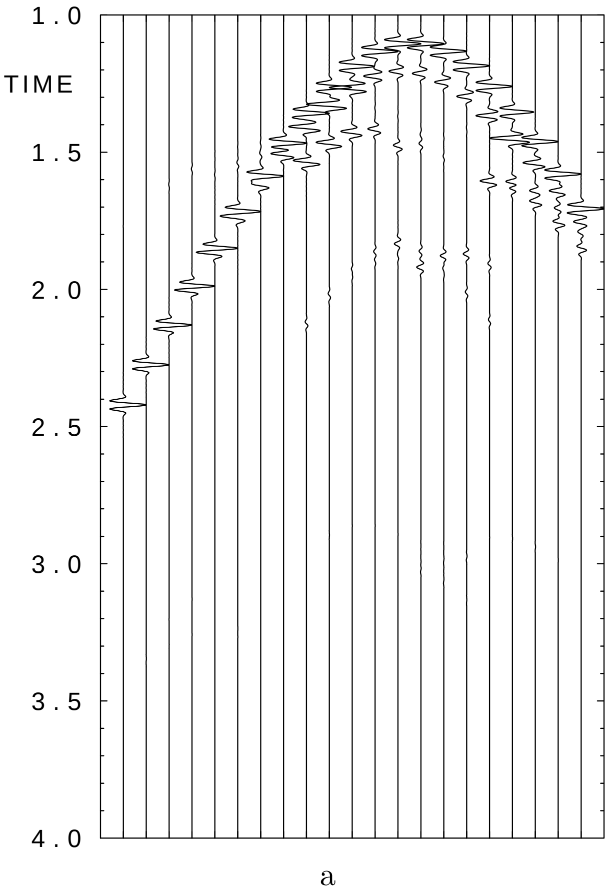

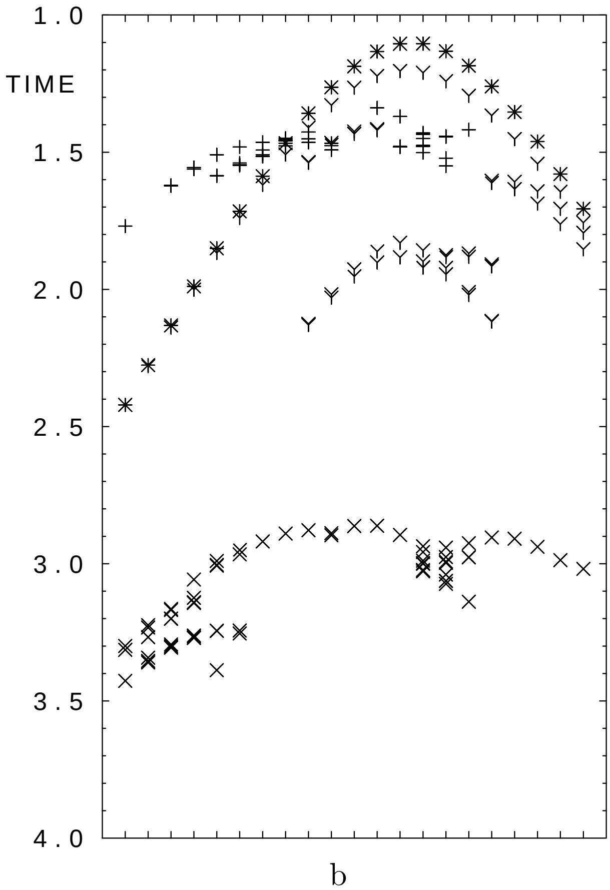

Figure 8. Shot located in the well, above the salt body, at a depth of 900m. **a**: Vertical components of synthetic seismograms of all computed elementary waves along the selected profile. The amplitudes of each trace are scaled according to the maximum amplitude of each trace. **b**: Travel times of the individual elementary waves along the selected profile. ' $*$ ' denotes the refracted wave, ' Y ' denotes the reflections from the top of salt, ' $+$ ' denotes the reflections from the bottom of salt and ' $\times$ ' denotes the reflections from the bottom interface.

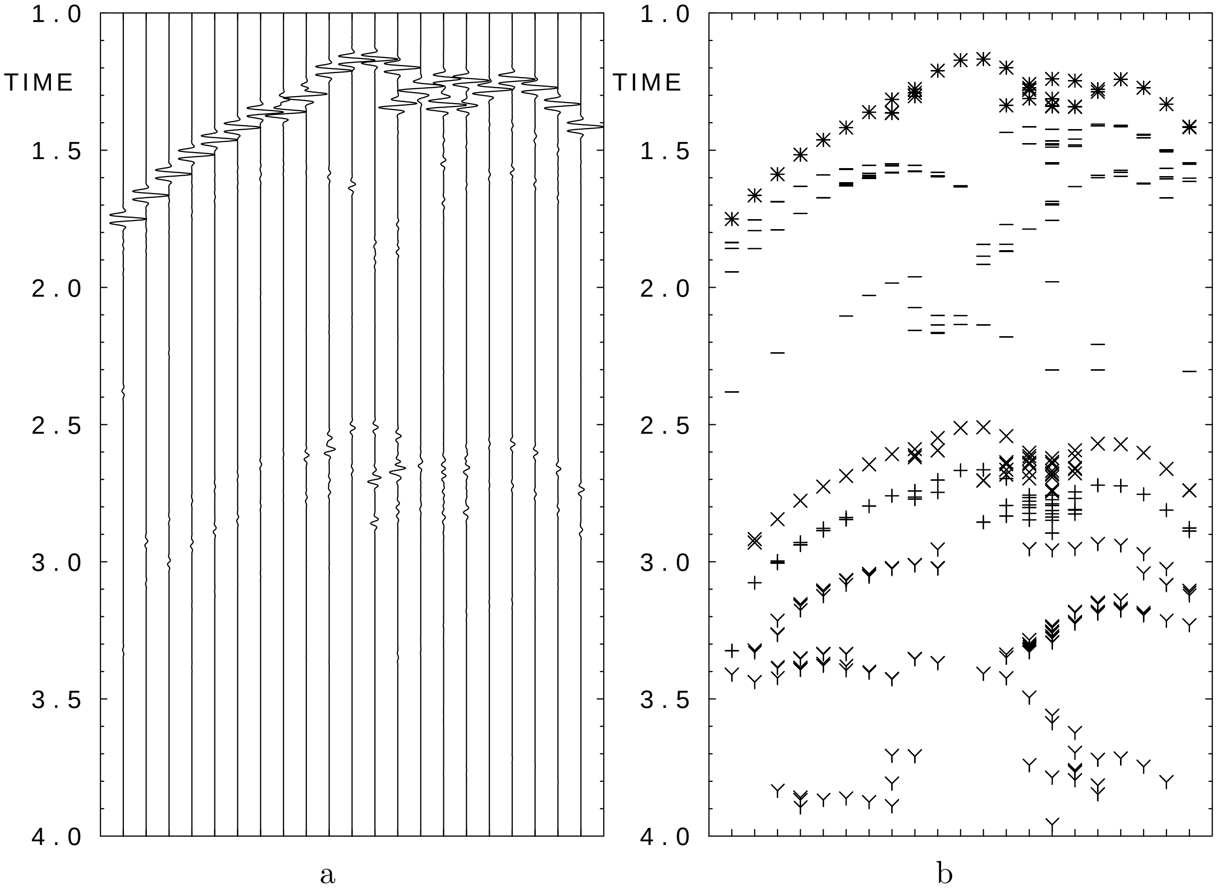

Figure 9. Shot located in the well, below the salt body, at a depth of 2300m. **a**: Vertical components of synthetic seismograms of all computed elementary waves along the selected profile. The amplitudes of each trace are scaled according to the maximum amplitude of each trace. **b**: Travel times of the individual elementary waves along the selected profile. ' $*$ ' denotes the refracted wave, ' $-$ ' denotes the multiple reflections from the top and bottom of salt, ' $\times$ ' denotes the reflections from the bottom interface, ' $+$ ' denotes the multiple reflections from the bottom of salt and bottom interface and ' Y ' denotes the multiple reflections from the top of salt and bottom interface.

CONCLUSIONS

The results of the calculations show that the smoothed SEG/EAGE Salt Model is suitable for two-point ray tracing. Computation and visualization of rays and travel times of the individual elementary waves is a great advantage of the ray tracing method and should help in studying problems in subsalt areas. The author hopes that computations for other shot and receiver configurations will be successful. A comparison of similar computations performed with a some precise method would be useful. This will be done in future.

The time of the computation for the shot located above the salt crest at the depth of 20m and for the shot in the well, above the salt, at the depth of 900m was approximately the same, 20 minutes on a PC equipped with an Athlon XP 3400+ processor. The computation time for the shot in the well, below the salt body, at the depth of 2300m is roughly three hours on the same PC. A more detailed description of the computation steps can be found in Bucha (2003, 2004).

ACKNOWLEDGMENTS

The author thanks Luděk Klimeš and Petr Bulant for their valuable comments and recommendations concerning this paper. The research was supported by the Grant Agency of the Czech Republic under Contract 205/04/1104, and by the members of the consortium "Seismic Waves in Complex 3-D Structures" (see "http://sw3d.mff.cuni.cz").

REFERENCES

Aminzadeh, F., Brac, J. and Kunz, T., 1997. 3-D Salt and Overthrust Models, SEG/EAGE 3-D Modeling Series No.1. Soc. Explor. Geophysicists, Tulsa.

Bucha, V., 2003. Ray tracing computations in the smoothed SEG/EAGE Salt Model. In: Seismic Waves in Complex 3-D Structures, Report 13, Dep. Geophys., Charles Univ., Prague: 241–248.

Bucha, V., 2004. Ray tracing computations in the smoothed SEG/EAGE Salt Model. Part 2: Sources in the well. In: Seismic Waves in Complex 3-D Structures, Report 14, Dep. Geophys., Charles Univ., Prague: 27–34.

Bucha, V., Bulant, P. and Klimeš, L., 2003. Velocity macro models. In: Extended Abstracts Book, EAGE/SEG Summer Research Workshop on 'Processing and imaging of seismic data' Using explicit or implicit velocity model information? (Trieste), Eur. Assoc. Geoscientists and Engr., Houten, T32 (4 pp.).

Bulant, P., 2001. Sobolev scalar products in the construction of velocity models - application to model Hess, to SEG/EAGE Salt Model, and to model Pluto 1.5. In: Seismic Waves in Complex 3-D Structures, Report 11, Dep. Geophys., Charles Univ., Prague: 133–159.

Bulant, P., 2002. Sobolev scalar products in the construction of velocity models: Application to model Hess and to SEG/EAGE Salt Model. Pure appl. Geophys., 159: 1487–1506.

Bulant, P., 2003. Constructing the SEG/EAGE 3-D Salt Model for ray tracing using Sobolev scalar products. In: Seismic Waves in Complex 3-D Structures, Report 13, Dep. Geophys., Charles Univ., Prague: 17–33.

Červený, V., Klimeš, L. and Pšenčík, I., 1988. Complete seismic-ray tracing in three-dimensional structures. In: Doornbos, D.J.(ed.), Seismological Algorithms, Academic Press, New York: 89–168.